Nonspecific Hydrophobic Interactions of a Repressor Protein, PhaR, with Poly[(*R*)-3-hydroxybutyrate] Film Studied with a Quartz Crystal Microbalance

Koichi Yamashita,*,†,‡ Miwa Yamada,§ Keiji Numata,|| and Seiichi Taguchi*,‡,§

Chemical Analysis Team, RIKEN Institute, 2-1 Hirosawa, Wako-shi, Saitama 351-0198, Japan, Polymer Chemistry Laboratory, RIKEN Institute, 2-1 Hirosawa, Wako-shi, Saitama 351-0198, Japan, Division of Biotechnology and Macromolecular Chemistry, Graduate School of Engineering, Hokkaido University, N13W8, Kita-ku, Sapporo, Hokkaido 060-8628, Japan, and Department of Innovative and Engineered Materials, Tokyo Institute of Technology, 4259 Nagatsuta, Midori-ku, Yokohama 226-8502, Japan

Received May 8, 2006

The gene expression for phasins (PhaP), which are predominantly polyhydroxyalkanoates (PHAs) granule-associated proteins, is regulated by a repressor protein of PhaR through the dual binding abilities of PhaR to the target DNAs and the granules. In this study, the binding functions of PhaR to poly[(*R*)-3-hydroxybutyrate] (P(3HB)) were investigated quantitatively by using a quartz crystal microbalance (QCM) technique. Adsorption of PhaR onto a melt-crystallized film of P(3HB) (cr-P(3HB)) was detected as a negative frequency shift of the QCM. The time course of the frequency changes observed for PhaR adsorption was composed of a quick frequency decrease at an initial stage and a subsequent slower frequency decrease for several hours, indicating multilayered adsorption of PhaR molecules onto cr-P(3HB). The initial rapid adsorption, which corresponds to direct adsorption of PhaR molecules onto a bare surface of cr-P(3HB), was a diffusion-controlled process. Strong interactions between PhaR and cr-P(3HB) were also observed as apparently irreversible adsorption. The comparative QCM measurement of PhaR adsorption onto various types of polymers with different aliphatic chemical structures revealed that PhaR was adsorbed onto the surfaces of polymers, including cr-P(3HB), mainly by nonspecific hydrophobic interactions. These results illustrate the high affinity and low specificity for adsorption of PhaR to P(3HB).

Introduction

Polyhydroxyalkanoates (PHAs) are typical biobased polymers that are produced from renewable resources.[1−5] Because of their biodegradable and thermoplastic properties, PHAs have attracted much attention for industrial applications as an ecofriendly material.[4] Various microorganisms synthesize PHAs as a carbon and energy storage material and accumulate them in the form of granules under nutrient-limited conditions. The PHA granules are covered with a layer composed of proteins and phospholipids.[6] The most abundant constituents of the layer are phasins (PhaP), which are amphipathic proteins of relatively small molecular size.[7−9] They have been found in various bacteria that accumulate PHAs.[7−19]

The production of PhaP is regulated through the synthesis of PHAs. The amount of PhaP affects the size and number of PHA granules, and is proportional to the contents of PHAs in bacteria.[7,10,11,13,16,20−22] The regulation mechanism of PhaP production has been revealed gradually by recent studies (Figure 1). We have been studying a repressor protein, PhaR, for the phasin PhaP gene expression by in vitro and heterogeneous expression systems.[16,23,24] DNase I footprinting revealed that the binding sites of PhaR are located upstream of the PhaP and

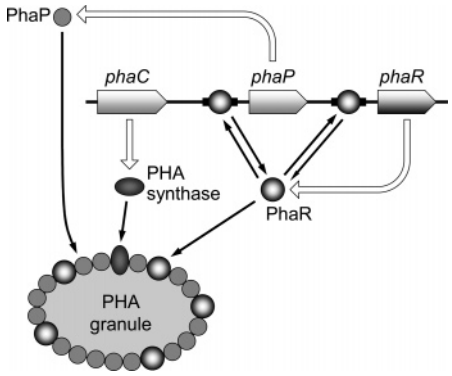

Figure 1. Regulation of PHA biosynthesis through the interactions of PhaR with upstream regions of PhaP gene (*phaP*) and PhaR gene (*phaR*), and PHA granule. *phaC* indicates the gene for PHA synthase. PhaP and *phaP* indicate a phasin protein and its gene, respectively.

PhaR genes in *Paracoccus denitrificans*, indicating that PhaR regulates the production of both PhaP and PhaR itself.[24] PhaR is also able to bind to poly[(*R*)-3-hydroxybutyrate] (P(3HB)) granules and 3HB oligomers, accompanied by dissociation of PhaR from PhaR−DNA complexes. In the postulated model, PhaR suppresses the production of PhaP and PhaR until synthesis of PHAs begin. Once PHA accumulation begins, PhaR dissociates from the target DNAs by binding to PHA, so as to allow the production of PhaP and PhaR.[24] Similar functions of PhaR were also reported by York et al. by using a PhaR gene knockout mutant of *Ralstonia eutropha*, which is a typical model organism to study the biosynthesis of short-chain-length PHA including P(3HB).[25] This regulation mechanism would suggest

* To whom correspondence should be addressed. (K.Y.) Phone: +81-48-467-8000. Fax: +81-48-462-4631. E-mail: koyama@riken.jp. (S.T.) Phone & Fax: +81-11-706-6610. E-mail: staguchi@eng.hokudai.ac.jp.
† Chemical Analysis Team, RIKEN Institute.
‡ Polymer Chemistry Laboratory, RIKEN Institute.
§ Hokkaido University.
|| Tokyo Institute of Technology.

10.1021/bm060442o CCC: $33.50
Published on Web 07/20/2006

that PhaR has two plausible domains capable of binding to hydrophilic DNA and hydrophobic PHAs. The interactions of PhaR with DNA have been extensively studied by means of molecular biological techniques such as gel shift assay and DNase I footprinting.[16,23,24,26,27] However, less is known concerning the binding functions of PhaR to PHAs.[24,27]

In this study, we have quantitatively investigated the binding functions of PhaR to P(3HB) film by using a quartz crystal microbalance (QCM) technique. QCM is recognized as a versatile technique to follow adsorption processes at a solid/liquid interface in chemical and biological studies. In previous papers, we have shown that adsorption of depolymerase to aliphatic polyesters can be followed continuously by QCM in the ng/cm^2 regime.[28−31] Although P(3HB) exists in an amorphous mobile state within intracellular native granules with assistance of amphipathic PhaP, the natural granules are denatured to a partially crystalline state by removal of, or damage to, the surface layer.[5,32] Therefore, it is impossible to reproduce the natural amorphous state in vitro. A melt-crystallized film of P(3HB) was used in this study. The present QCM study has quantitatively revealed the characteristics of the binding functions of PhaR to the P(3HB) film.

Experimental Section

Materials. P(3HB), poly(L-lactide) (PLLA), polyethylene (PE), and polystyrene (PS) were obtained from ICI, Polyscience, Aldrich, and Nishio, respectively. P(3HB) and PLLA were purified by reprecipitation with methanol from chloroform solution and dried in vacuo. PE and PS were used as received. The number-average molecular weight (M_n) and molecular weight distribution (M_w/M_n) of the polymers were 697 000 and 2.6 for P(3HB), 410 000 and 1.7 for PLLA, 7700 and 4.5 for PE, and 1 380 000 and 1.3 for PS, respectively.

Production and Purification of PhaR. A plasmid pTV119N::*phaR* was digested with *Nco*I and *Hin*dIII and blunted with T4 DNA polymerase. Then, the digested DNA fragment including the PhaR gene was inserted into the expression vector, pQE30 (Qiagen), that was digested with *Bam*HI and *Hin*dIII and blunted with T4 DNA polymerase. The resultant plasmid is referred to as pQE::*phaR* (Figure 2A). Expression of the PhaR gene was driven under the T5 promoter that is inducible with isopropyl-β-D-thiogalactopyranoside (IPTG). The constructed plasmid was introduced into *Escherichia coli* BL21(DE3) harboring pREP-4 (Qiagen), which encodes the *lacI*^{q} gene. Transformants were grown in 1200 mL of Luria-Bertani medium containing ampicillin (100 μg/mL) and kanamycin (50 μg/mL). They were cultivated at 30 °C until the OD_{600} of the culture reached 0.5. After the addition of IPTG (final concentration of 1 mM), the transformants were grown for an additional 5 h. The cells were then harvested and washed with chilled buffer A (50 mM sodium phosphate (pH 8.0) containing 300 mM NaCl and 10 mM imidazole) and were suspended in 60 mL of the same buffer. The suspension was stored at −80 °C until use.

The suspension was thawed on ice and disrupted by sonic oscillation (Ohtake Works, Tokyo, Japan) on ice. The cell debris was then removed by centrifugation at 15 000*g* for 60 min at 4 °C, and the supernatant was collected for purification. The experiments were carried out at 4 °C throughout the purification steps. The crude extract was shaken gently with nickel−nitrilotriacetic acid agarose (Qiagen) for 1 h. The mixture was then poured onto a column. The column was washed with buffer A containing 20 mM imidazole, and then, a His-tagged protein was eluted with buffer A containing 250 mM imidazole. The eluates containing PhaR were dialyzed with 10 mM HEPES (pH 7.4) containing 15 mM NaCl and 3 mM EDTA and stored at −80 °C. Protein concentration was determined using a Bio-Rad Protein Assay Kit with bovine serum albumin as the standard. Proteins were separated by sodium dodecyl sulfate (SDS)-12.5% polyacrylamide gel electrophoresis and stained with Coomassie brilliant blue (CBB) R-250 as described by Laemmli (Figure 2B).[33]

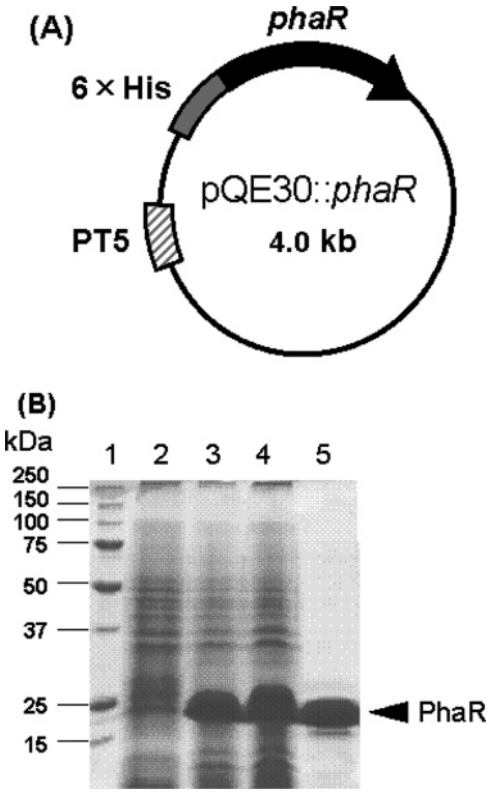

Figure 2. (A) Structure of expression vector for *phaR*. PT5 and 6 × His denote T5 promoter and His-tag coding region, respectively. The *phaR* gene encodes the PhaR from *Paracoccus denitrificans*. (B) Purification profiles of recombinant PhaR. Proteins were separated in a SDS-12.5% polyacrylamide gel and stained with CBB R-250. Lane 1, molecular mass standard proteins; lane 2, total cellular proteins of *E. coli* BL21(DE3) harboring pQE30 and pREP-4; lane 3, total cellular proteins of *E. coli* BL21(DE3) harboring pQE30-*phaR* and pREP-4; lane 4, soluble protein fraction of *E. coli* BL21(DE3) harboring pQE30-*phaR* and pREP-4; lane 5, purified PhaR by nickel−nitrilotriacetic acid agarose (16 μg).

Preparation of Thin Films. QCM oscillators were washed with a freshly prepared Piranha solution of H_2O_2/H_2SO_4 (1/3 v/v) and were rinsed several times with Milli-Q water. (Caution: Piranha solution is very oxidative and dangerous, and direct contact should be avoided.) Thin films of P(3HB), PLLA, and PS were prepared on the QCM oscillators by casting chloroform solutions (1.0−1.5 wt %) of the polymers on a spin-coater (MOC Co., Ltd.; ME−300) at 4000 rpm under dry air. For preparation of a PE thin film, *p*-xylene solution (1.0 wt %) of PE was spin-cast on the oscillator. Melt-crystallized films of P(3HB) (cr-P(3HB)) and PLLA (cr-PLLA) were prepared by melting their spin-cast films at 200 and 220 °C for 30−60 s followed by isothermal crystallization at 110 °C and 120 °C for 1 day, respectively. For preparation of an amorphous PLLA film (am-PLLA), the spin-cast film was melted at 220 °C for 30−60 s and then quenched immediately at 0 °C. By using transmission electron microscopy, it was found that the PLLA thin film showed no electron diffraction spots after quenching.[29] The average surface roughnesses (R_a) of the films estimated by atomic force microscopy (AFM) in a 1 × 1 μm^2 area were 2.0 nm for cr-P(3HB), 5.4 nm for cr-PLLA, 0.54 nm for am-PLLA, 1.4 nm for spin-cast PS (sp-PS), and 1.4 nm for spin-cast PE (sp-PE), respectively. To determine the thickness of the films, films that had been scratched by a wire were analyzed by AFM. The thicknesses were ca. 100 nm for cr-P(3HB), cr-PLLA, and am-PLLA films, and ca. 40 nm for sp-PS and sp-PE films, respectively.

QCM Analysis. A commercially available QCM setup of QCA-922 (SEIKO EG&G) was equipped with a homemade cell with an inner volume of ca. 0.2 mL that was designed to reduce fluctuation of signals due to injection of the sample solution (Figure 3). Its temperature was thermostated at 25.0 ± 0.1 °C by circulating water. The oscillator was

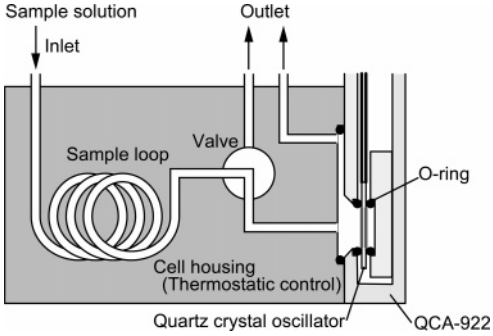

Figure 3. Schematic illustration of the homemade cell housing of the QCM setup.

a polished 9 MHz AT-cut quartz crystal, on both sides of which Au electrodes were deposited (area size: 0.196 $cm^2 \times 2$). The mean roughness of the electrode surface was estimated to be 1.2 nm (30×30 μm) by AFM. When frictional changes of the oscillator are negligible, a frequency shift of 1.0 Hz corresponds to a mass change of 1.0 ng on the electrode (0.196 cm^2) according to the Sauerbrey equation.[34,35] Sample solutions were set to the measuring temperature in the sample loop for 10 min before injection into the inner cell by gravitational flow. After stabilization of the QCM in 10 mM HEPES buffer solution (pH 7.4) containing 150 mM NaCl, the reaction was initiated by replacing the buffer solution with the PhaR solution. The total volume used for replacement was 1.25 mL. Resonant frequency and resonant resistance were monitored simultaneously to evaluate the influence of frictional changes.

AFM Observations. Morphologies of the thin films on a QCM oscillator and PhaR on am-PLLA films were observed by dynamic force mode (tapping mode) AFM (SPI3800/SPA400, SII NanoTechnology Inc.) in air at 25 °C. A rectangular Si cantilever with spring constants of 2.1 N/m was used for the AFM observation with a light tapping force (the set-point amplitude/free oscillating amplitude = 0.8−0.9). The scan rate was 0.8 Hz, and the scan angle was set to −90°. Height and phase images were recorded simultaneously. For observation of PhaR adsorption layers, an am-PLLA film on the oscillator was immersed for 10 min in 1.5 mL of the buffer solution (pH 7.4) containing 20 μg/mL PhaR, and then, the film was washed gently with Milli-Q water before AFM measurements.

Results and Discussion

Using the recombinant production system and affinity purification procedures (see Experimental Section), recombinant PhaR protein was efficiently purified to be homogeneous on SDS−polyacrylamide gel electrophoresis (Figure 2) with a yield of approximately 7 mg from 1200 mL of culture medium.

The interactions of PhaR with the melt-crystallized film of P(3HB) (cr-P(3HB)) were monitored by QCM. Frequency changes observed for the interactions at various PhaR concentrations are summarized in Figure 4. The frequency decreased quickly immediately after injection of the PhaR solution into the QCM cell, as shown in Figure 4A. Then, a slower decrease in the frequency was observed for several hours to reach constant ΔF values (Figure 4B). The resonant resistance did not change during the measurements (data not shown), indicating that the frictional changes of the QCM on addition of PhaR were negligibly small. Therefore, a negative shift in the frequency indicates directly a mass uptake on the QCM oscillator,[34,35] and the frequency changes shown in Figure 4 can be assigned to adsorption of PhaR onto the P(3HB) film.

The characteristic time profiles in Figure 4 suggest multilayered adsorption of PhaR onto the P(3HB) film. The saturated amount of PhaR in monolayer adsorption can be calculated from its molecular weight. By taking account of hydration, we can assume that the effective specific volume of a protein is ca. 1 cm^3/g in aqueous solution.[36] Then, the volume of one PhaR molecule is estimated to be ca. 37 nm^3 from its molecular weight of 22 kDa.[23] If the protein particle is spherical, the radius of the protein is 2.1 nm, and the cross-sectional area is 13.9 nm^2. Then, the saturated amount of the monolayer of PhaR on the QCM is calculated to be 239 ng/cm^2 by assuming hexagonal packing of circles. Because the calculated amount corresponds to the frequency shift of ca. −47 Hz, the slower adsorption process observed under the conditions of [PhaR] ≥ 10 μg/mL can be attributed to multilayered adsorption of PhaR onto the first PhaR layer.

The multilayered adsorption of PhaR was supported by AFM observations of the adsorption layer of PhaR on the films. Although we could not directly identify multilayered adsorption of the PhaR molecules on cr-P(3HB) film by AFM due to the very rough surface of the film, the flat and smooth surface of an amorphous PLLA (am-PLLA) film permitted the observation of each layer of the stacked PhaR molecules. Figure 5 shows the AFM images and their cross-sectional data for the film before and after reaction with 20 μg/mL PhaR solution for 10 min, at which the slower adsorption of PhaR was in progress. The PhaR layer adsorbed on the film surface emerged clearly

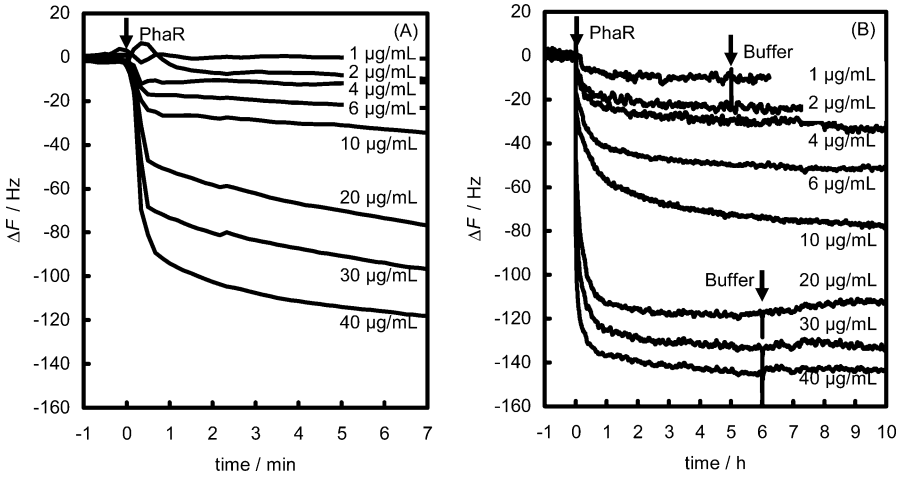

Figure 4. Time courses of frequency changes (ΔF) observed for (A) the initial part and (B) the whole of the adsorption reaction of PhaR onto P(3HB) film at 25 °C, in which the PhaR solution in the QCM cell was replaced with the buffer solution after adsorption attained equilibrium. The arrows denote the injection point of the PhaR solution and the replacement point, respectively. The concentrations of PhaR are shown in the figure.

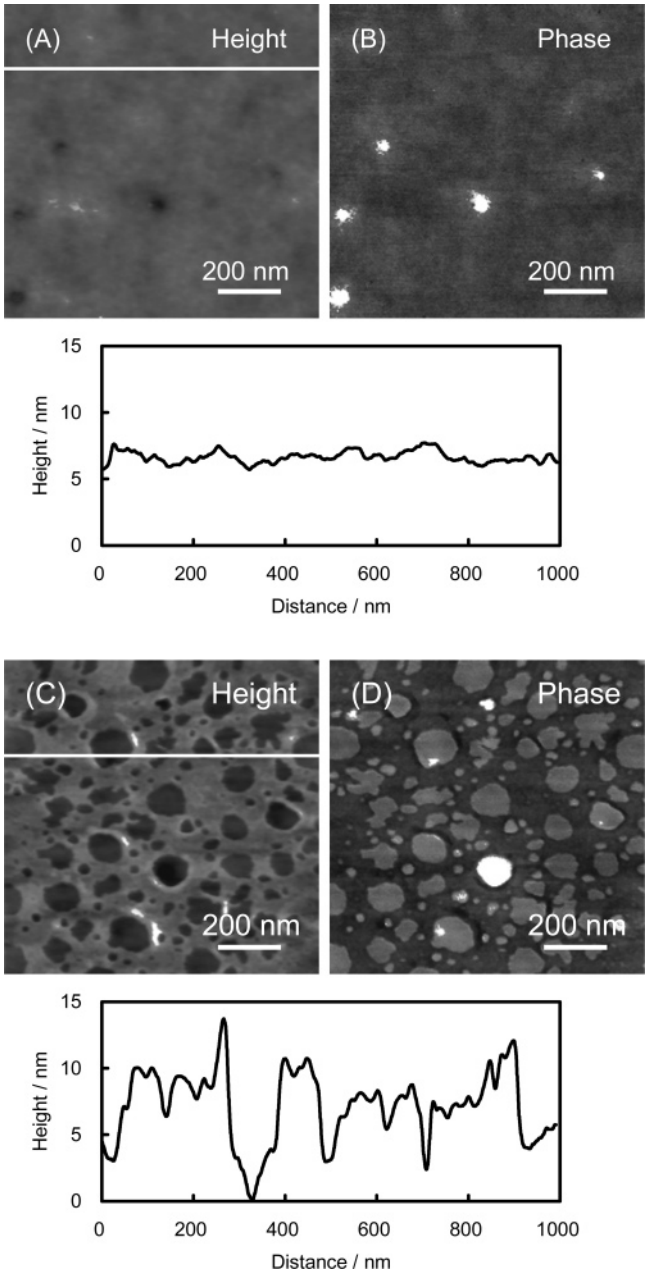

Figure 5. AFM height and phase images of PLLA amorphous film (A and B) and PhaR adsorbed on the film surface after reaction with 20 μg/mL PhaR solution for 10 min (C and D). Cross-sectional data were estimated at the white line regions.

with a characteristic morphology, as shown in Figure 5C,D. The uppermost layer of adsorbed PhaR does not cover the whole surface, and there are many basins that correspond to lower PhaR layers. A swollen part resulting from additional PhaR adsorption can also be observed on the uppermost layer. As can be seen from the cross-sectional data, the height of each layer seems to be about 4−5 nm, which corresponds to the diameter of one PhaR molecule as calculated above. These observations support the multilayered adsorption of PhaR.

However, multilayered adsorption of PhaR observed in the simplified QCM system would be apparently disadvantageous in considering its regulating function in PHA synthesis. PhaR has been shown to regulate the expressions of the PhaP and PhaR genes by its dual binding ability to the target DNAs and PHA granules.[16,23,24,26,27] When the cells begin to synthesize PHAs, PhaR molecules bind to polymer chains with dissociation from DNA, which results in synthesis of PhaP and PhaR for

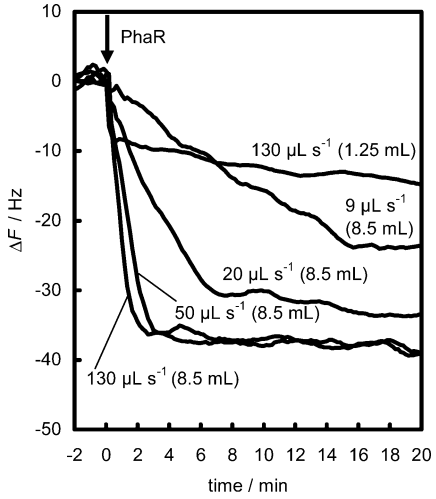

Figure 6. Effects of the injection conditions of 2 μg/mL PhaR solution on the frequency changes during adsorption of PhaR onto P(3HB) film at 25 °C. The injection rates are shown in the figure with the injection volume in parentheses.

granule formation. PhaP is sufficiently supplied during the growth of granules because the cytoplasmic concentration of PhaR remains low, preventing binding to the genes by continuous tight binding to the granules. When the granule growth has come to a limit, no additional space for adsorption of PhaR is available on the granule surface, after which free PhaR molecules bind to the upstream elements and repress both PhaP and PhaR gene expression. Accordingly, PhaR needs to bind quantitatively to the PHA granules to synchronize the production of PhaP and PhaR with the growth of PHA granules. If PhaR molecules are adsorbed onto the PHA surface as a multilayer, the adsorbed amount of PhaR would not directly reflect the size of the granules, because additional adsorption of PhaR molecules onto the first layer of adsorbed PhaR is independent of the size of the granules. Although the present results suggest the possibility of multilayered adsorption of PhaR, PhaR might be adsorbed as a monolayer in a cell because the actual cytoplasmic concentration of PhaR would be very low compared with the PhaR concentration in the present experiment. In addition, most of the surface of the PHA granules is covered with PHA synthases and PhaP, and the content of PhaR is very low. Therefore, the amphiphilic property of PhaP may prevent additional binding of PhaR onto the first monolayer on granules. This assumption is supported by the previous results that native PHA granules, which were covered with PhaP or other nonspecific proteins, did not cause the dissociation of PhaR from PhaR−DNA complexes, but artificial P(3HB) granules and 3HB oligomers caused dissociation.[24]

To characterize PhaR adsorption onto the bare surface of P(3HB) film, the effects of the injection rate and the injection volume of the PhaR solution on the frequency changes were examined under the conditions of [PhaR] = 2 μg/mL, at which multilayered adsorption of PhaR onto the P(3HB) surface was negligible. As shown in Figure 6, rapid adsorption was observed during the sample injection, and the adsorption process became slower after completion of the injection. With a constant injection volume of 8.5 mL, the rate of the rapid adsorption increased with increasing injection rate and reached a constant rate at injection rates faster than 50 μL/s. The adsorbed amounts of PhaR by the initial fast adsorption also increased with increasing injection rates and reached a limiting value of ca −37 Hz at injection rates faster than 50 μL/s. Because this saturated amount is close to the above-mentioned shift of −47

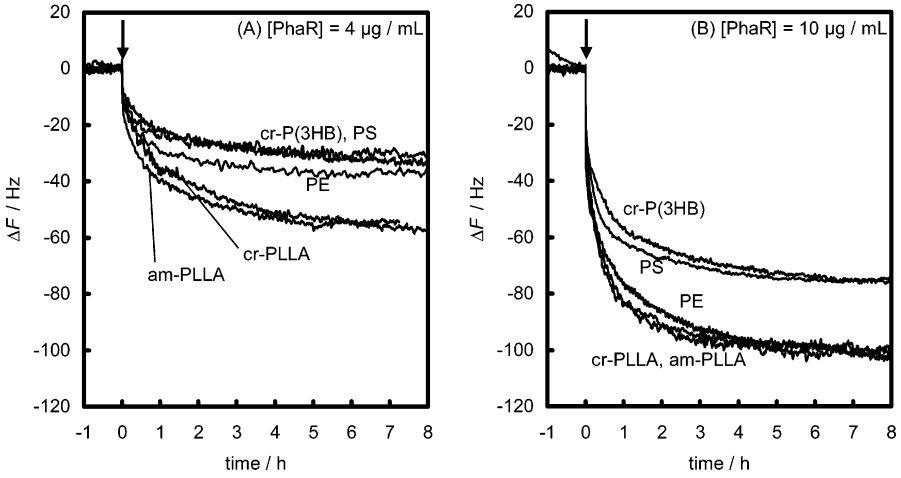

Figure 7. Time courses of frequency changes (ΔF) observed during adsorption of PhaR onto various polymer films (cr-P(3HB), cr-PLLA, am-PLLA, PS, and PE) at (A) [PhaR] = 4 μg/mL and (B) 10 μg/mL. The arrow denotes the injection point of the PhaR solution.

Hz calculated for the saturated amount of PhaR in monolayer adsorption, the film surface would be covered with a monolayer of PhaR molecules. The facts suggest that the initial fast adsorption is monolayer adsorption of PhaR onto the P(3HB) surface. Consistent with this assumption, the smaller injection volume of 1.25 mL became depleted before the surface was covered with PhaR molecules; however, the initial adsorption rate was the same.

Dependence of the rate of the initial adsorption process on the injection rate clearly indicates that the initial rapid adsorption resulted from the injection flow of the sample solution. In other words, the injection flow accelerated supply of PhaR molecules to the bare film surface to accelerate adsorption of PhaR. Saturation of the adsorption rate observed at injection rates grater than 50 μL/s indicates sufficient supply of PhaR molecules to the film surface by the fast injection flow. Thus, adsorption of PhaR is a diffusion-controlled process, in which the adsorption rate of PhaR onto the P(3HB) film depends on transport of PhaR molecules to the vicinity of the film surface from the bulk solution. The results suggest a high affinity of PhaR for the P(3HB) film.

Strong interactions between PhaR and P(3HB) were also observed as an apparent irreversibility of adsorption. When the PhaR solutions in the QCM cell were replaced with buffer solutions containing no PhaR after adsorption attained equilibrium, no frequency changes were observed, as shown in Figure 4B, indicating that the adsorbed PhaR molecules did not come off the film surface. In other words, adsorption of PhaR onto the P(3HB) film is irreversible over the present time scale of several hours. Irreversible adsorption of PhaR to PHAs was also suggested qualitatively in the previous study[24] to examine the binding ability of PhaR to P(3HB). In that experiment, P(3HB) granules incubated with PhaR were washed twice with buffer followed by treatment with denaturing buffer to remove PhaR from the granules. The recovered PhaR in the solution was then detected as the granule-associated PhaR by SDS−PAGE. These procedures imply not only the tight binding ability of PhaR to P(3HB) but also the apparent irreversibility of the PhaR binding.

Despite the apparent irreversibility of the PhaR binding, the adsorbed amount of PhaR after several hours depended on the PhaR concentration, as can be seen from Figure 4B. This can be explained by taking account of deformation of the PhaR molecules by adsorption.[37] Because protein molecules are large and soft, their strong and multiple interactions with a surface and neighboring proteins can result in deformation of the protein molecules upon adsorption. When deformation of the adsorbed PhaR molecule competes with subsequent adsorption of neighboring molecules, deformation can be hindered by the neighboring molecules so as to be closely packed. Thus, the number of PhaR molecules on the film might increase with PhaR concentration.

The mode of adsorption of PhaR was investigated in terms of its substrate specificity for adsorption to various polymer films. Figure 7 shows the time course of the frequency changes observed for the adsorption reaction of PhaR to am-PLLA films, melt-crystallized PLLA (cr-PLLA) films, spin-cast PS (sp-PS) films, and spin-cast PE (sp-PE) films in addition to cr-P(3HB) films at [PhaR] = 4 and 10 μg/mL. PhaR was adsorbed onto all the films examined with somewhat different adsorption rates. The adsorption rate for the cr-P(3HB) film was almost the same as that for the sp-PS film but slower than those of the am- and cr-PLLA films and the sp-PE film. The total amounts of adsorbed PhaR in equilibrium could be estimated from the frequency shifts at the time when the frequency changes reached constant values. The total amounts of PhaR adsorbed to cr-P(3HB) and sp-PS were smaller than those to am- and cr-PLLA and sp-PE, in accordance with the tendency of the adsorption rates. The fact that the affinity of PhaR to cr-P(3HB) is not necessarily higher than those to other films indicates that PhaR is adsorbed onto P(3HB) mainly by nonspecific hydrophobic interactions. The origin of different affinities of PhaR to various polymer films is not clear at present because, as well as the chemical structures of the polymers, the mesoscopic morphologies such as surface roughness of the films can affect the apparent interactions between polymer films and proteins. The AFM images observed for the polymer films used in this study showed very different morphologies (data not shown), and the correlation between the average surface roughness (R_a) of the films and the affinities to PhaR was not straightforward. Therefore, an extensive and complex study would be required for more precise understanding of adsorption behaviors of PhaR onto diverse polymer films. Such a detailed study is under way in this laboratory.

Conclusions

Adsorption of PhaR to P(3HB) film was quantitatively followed by QCM. The adsorption process consisted of a rapid adsorption at an initial stage and a subsequent slower adsorption, indicating multilayered adsorption of PhaR molecules onto the film. The direct adsorption of PhaR onto the bare surface of

the P(3HB) film was a diffusion-controlled process. The strong affinity of PhaR to P(3HB) also appears to be an apparently irreversible adsorption. The observations of PhaR adsorption onto various types of polymers revealed that PhaR was adsorbed onto the polymer surfaces mainly by nonspecific hydrophobic interactions.

Acknowledgment. This work has been supported by grants for Ecomolecular Science Research from the RIKEN Institute and a Grant-in-Aid for Scientific Research (no. 16550139 to K.Y. and no. 17360392 to S.T.) from the Ministry of Education, Culture, Sports, Science, and Technology, Japan. K.N. is a recipient of JSPS Research Fellowships.

References and Notes

(1) Anderson, A. J.; Dawes, E. A. *Microbiol. Rev.* **1990**, *54*, 450.
(2) Doi, Y. *Microbial Polyesters*; VCH Publishers: New York, 1990.
(3) Sudesh, K.; Abe, H.; Doi, Y. *Prog. Polym. Sci.* **2000**, *25*, 1503.
(4) Doi, Y., Steinbüchel, A., Eds. *Biopolymer. Polyester III*; Wiley-VCH: Weinheim, 2002; Vol. 4.
(5) Lenz, R. W.; Marchessault, R. H. *Biomacromolecules* **2005**, *6*, 1.
(6) Pöter, M.; Steinbüchel, A. *Biomacromolecules* **2005**, *6*, 552.
(7) Steinbüchel, A.; Aerts, K.; Babel, W.; Föellner, C.; Liebergesell, M.; Madkour, M. H.; Mayer, F.; Pieper-Fürst, U.; Pries, A.; Valentin, H. E.; Wieczorek, R. *Can. J. Microbiol.* **1995**, *41* (Suppl. 1), 94.
(8) Steinbüchel, A.; Valentin, H. E. *FEMS Microbiol. Lett.* **1995**, *128*, 219.
(9) Wieczorek, R.; Steinbüchel, A.; Schmidt, B. *FEMS Microbiol. Lett.* **1996**, *135*, 23.
(10) Pieper-Fürst, U.; Madkour, M. H.; Mayer, F.; Steinbüchel, A. *J. Bacteriol.* **1994**, *176*, 4328.
(11) Pieper-Fürst, U.; Madkour, M. H.; Mayer, F.; Steinbüchel, A. *J. Bacteriol.* **1995**, *177*, 2513.
(12) Liebergesell, M.; Steinbüchel, A. *Biotechnol. Lett.* **1996**, *18*, 719.
(13) Wieczorek, R.; Pries, A.; Steinbüchel, A.; Mayer, F. *J. Bacteriol.* **1995**, *177*, 2425.
(14) Schembri, M. A.; Woods, A. A.; Bayly, R. C.; Davies, J. K. *FEMS Microbiol. Lett.* **1995**, *133*, 277.
(15) Pöter, M.; Müller, H.; Reinecke, F.; Wieczorek, R.; Fricke, F.; Bowien, B.; Friedrich, B.; Steinbüchel, A. *Microbiology* **2004**, *150*, 2301.
(16) Maehara, A.; Ueda, S.; Nakano, H.; Yamane, T. *J. Bacteriol.* **1999**, *181*, 2914.
(17) McCool, G. J.; Cannon, M. C. *J. Bacteriol.* **1999**, *181*, 585.
(18) Valentin, H. E.; Stuart, E. S.; Fuller, R. C.; Lenz, R. W.; Dennis, D. *J. Biotechnol.* **1998**, *64*, 145.
(19) Prieto, M. A.; Bühler, B.; Jung, K.; Witholt, B.; Kessler, B. *J. Bacteriol.* **1999**, *181*, 858.
(20) York, G. M.; Stubbe, J.; Sinskey, A. J. *J. Bacteriol.* **2001**, *183*, 2394.
(21) York, G. M.; Junker, B. H.; Stubbe, J.; Sinskey, A. J. *J. Bacteriol.* **2001**, *183*, 4217.
(22) Jossek, R.; Reichelt, R.; Steinbüchel, A. *Appl. Microbiol. Biotechnol.* **1998**, *49*, 258.
(23) Maehara, A.; Doi, Y.; Nishiyama, T.; Takagi, Y.; Ueda, S.; Nakano, H.; Yamane, T. *FEMS Microbiol. Lett.* **2001**, *200*, 9.
(24) Maehara, A.; Taguchi, S.; Nishiyama, T.; Yamane, T.; Doi, Y. *J. Bacteriol.* **2002**, *184*, 3992.
(25) York, G. M.; Stubbe, J.; Sinskey, A. J. *J. Bacteriol.* **2002**, *184*, 59.
(26) Pöter, M.; Müller, H.; Steinbüchel, A. *Microbiology* **2005**, *151*, 825.
(27) Pöter, M.; Madkour, M. H.; Mayer, F.; Steinbüchel, A. *Microbiology* **2002**, *148*, 2413.
(28) Kikkawa, Y.; Yamashita, K.; Hiraishi, T.; Kanesato, M.; Doi, Y. *Biomacromolecules* **2005**, *6*, 2084.
(29) Yamashita, K.; Kikkawa, Y.; Kurokawa, K.; Doi, Y. *Biomacromolecules* **2005**, *6*, 850.
(30) Yamashita, K.; Funato, T.; Suzuki, Y.; Teramachi, S.; Doi, Y. *Macromol. Biosci.* **2003**, *3*, 694.
(31) Yamashita, K.; Aoyagi, Y.; Abe, H.; Doi, Y. *Biomacromolecules* **2001**, *2*, 25.
(32) Jendrossek, D.; Handrick, R. *Annu. Rev. Microbiol.* **2002**, *56*, 403.
(33) Laemmli, U. K. *Nature (London)* **1970**, *227*, 680.
(34) Sauerbrey, Z. *Z. Phys.* **1959**, *155*, 206.
(35) Höök, F.; Kasemo, B.; Nylander, T.; Fant, C.; Sott, K.; Elwing, H. *Anal. Chem.* **2001**, *73*, 5796.
(36) Barrow, G. M. In *Physical Chemistry*, fifth ed.; McGraw-Hill: New York, 1988; Chapter 20.
(37) Malmsten, M., Ed. *Biopolymers at Interfaces*, 2nd ed.; McGraw-Hill: New York, 2003.

BM060442O